SINGLE FRAME PROFILOMETRY WITH RAPID PHASE DEMODULATION ON COLOUR-CODED FRINGES

YEE CONG KAI

UNIVERSITI SAINS MALAYSIA

2019

SINGLE FRAME PROFILOMETRY WITH RAPID PHASE DEMODULATION ON COLOUR-CODED FRINGES

by

YEE CONG KAI

Thesis submitted in fulfilment of the requirements for the degree of Master of Science

July 2019

ACKNOWLEDGEMENT

First of all, I would like to express my deepest and sincere gratitude to my supervisor, Ir. Dr. Yen Kin Sam for his guidance and support in the development and completion of this study. Without his thoughtful guidance and critical comments throughout the study, this thesis would not be materialized. Besides, I would also like to thank Mr. Mohd Fahmi Peter@Mohd Fauzi for teaching me on how to carry out the 3D profiling using the coordinate measuring machine. I am also grateful for the generosity of Numeral Engineering Sdn. Bhd. in providing fabrication service free of charge for the research. The experiments and verification of the research works would not progress so smoothly without their helps. I would also like to express my appreciation for the financial support given by Ministry of Higher Education, Malaysia and Universiti Sains Malaysia through MyBrain15, Exploratory Research Grant Scheme and Bridging Grant respectively. Last but not least, I am very grateful to my family members for their continuous support and encouragement in all aspects of my life.

TABLE OF CONTENTS

Page

LIST OF TABLES

Page

LIST OF FIGURES

Page

LIST OF ABBREVIATIONS

3D	Three-dimensional
CCD	Charge-coupled device
CMM	Coordinate measuring machine
CPU	Central processing unit
DFPP	Digital fringe projection profilometry
EMD	Empirical mode decomposition
FTP	Fourier transform profilometry
HSV	Hue, saturation, value
MAPE	Mean absolute percentage phase error
MEMS	Micro-Electro-Mechanical Systems
MXAPE	Maximum absolute percentage phase error
PCA	Principle component analysis
RAM	Random-access memory
RGB	Red, green, blue
WTP	Wavelet transform profilometry
XGA	Extended graphics array

LIST OF SYMBOLS

B	Length of De Bruijn's sequence
E	Local extrema
e	Phase errors
h	Height map
H	Hue value
h_c	Height of camera optical centre from reference plane
h_o	Height of known object
h_p	Height of projector optical centre from reference plane
i	Image coordinate (second dimension)
I_{ideal}	Ideal fringe image
I_{input}	Input fringe image
I_n	Fringe image of current loop during fringe image calibration
I_{n+1}	Fringe image of next loop during fringe image calibration
I_{output}	Output fringe image
j	Current pixel coordinate
j	Image coordinate (first dimension)
j_n	Coordinate of the nearest local extrema that is smaller than current pixel coordinate
j_{n+1}	Coordinate of the nearest local extrema that is larger than current pixel coordinate
k	Number of independent codes
K	Fringe order map
L	Lower limit of filtered fringe intensity
l_n	Local minima of filtered fringe intensity
L^p	Lebesgue spaces

n	Number of consecutive code being evaluated at a time
N	Normalised fringe intensity
q	Distance between camera optical axis and projector optical axis
Q	Image projection and image acquisition process
R	Resizing process
U	Upper limit of filtered fringe intensity
u_n	Local maxima of filtered fringe intensity
V	Fringe intensity
v_1	Distance on reference plane
v_2	Distance on object surface
x	Coordinate of object (first dimension)
y	Coordinate of object (second dimension)
z	Coordinate of object (third dimension)
ΔE	Difference between acquired fringe pattern image and ideal fringe pattern image
ΔV	Local gradient of fringe intensity
φ	Normalised absolute phase map
ϕ	Wrapped phase map

PROFILOMETRI DALAM SATU IMEJ DENGAN DEMODULASI FASA PESAT PADA JALUR BERKOD WARNA

ABSTRAK

Profilometri unjuran pinggir digital (DFPP) ialah sejenis teknik pengukuran tiga dimensi (3D) yang boleh mengukur seluruh permukaan pada masa yang sama tanpa sentuhan. Dengan kebolehan untuk menjalankan pengukuran dinamik yang berkejituan tinggi pada kadar bingkai video yang setinggi 4000 Hz, teknik ini amat berguna dalam bidang bioperubatan, pemeriksaan industry dan pemeliharaan kerja seni dan warisan budaya. Salah satu cabaran dalam *DFPP* adalah untuk meningkatkan kelajuan pengukuran supaya daya pemprosesan dan kadar pengukuran dinamik pada permukaan dapat ditingkatkan. Dalam kerja ini, kebolehgunaan corak tayangan yang dikodkan mengikuti urutan De Bruijn dan ralat fasa yang disebabkan oleh ketidaklinearan gama dan cakap silang warna telah dikaji. Permudahan model geometri dengan menggunakan sudut kecondongan penayangan dalam projector juga dikaji dalam tesis ini. Dengan itu, satu algoritma analisa pinggir telah dicadangkan bagi corak tayangan yang dikodkan mengikuti urutan *De Bruijn* untuk mengelakkan teknik-teknik *phase unwrapping* yang kurang teguh dan mengambil masa. Satu algoritma pembetulan ralat fasa dan geometri model yang dipermudahkan juga dicadangkan untuk mengurangkan ralat fasa dan bilangan parameter model yang diperlukan. Tiga eksperimen telah dijalankan untuk (i) mengesahkan kebolehgunan sistem *single-frame profilometry* yang dicadangkan, (ii) mengesahkan kebolehgunan algoritma pembetulan ralat fasa yang dicadangkan dan (iii) menbandingkan hasil pengukuran oleh kaedah yang dicadangkan dengan mesin pengukur koordinat (CMM) CRYSTA-Plus M Series untuk mengetahui perbezaan prestasi antara dua kaedah

tersebut. Hasil eksperimen menunjukkan bahawa kaedah yang dicadangkan dapat membentuk semula permukaan objek secara tekal dengan hanya satu gambar. Algoritma pembetulan ralat fasa juga terbukti dapat mengurangkan ralat fasa pada permukaan rujukan dari (1.08 ± 2.32) % kepada (0.73 ± 0.46) % pada tahap keyakinan 95% dalam 8 lelaran secara purata dan menghasilkan permukaan objek dibentuk semula yang lebih licin pada penglihatan. Perbandingan dengan mesin pengukur koordinat menunjukkan bahawa perbezaan antara profil dibina semula oleh kaedah yang dicadangkan dan profil dibina semula oleh mesin pengukuran koordinat pada permukaan bilah kipas adalah 2.63 mm secara purata dan selang keyakinan pada tahap keyakinan 95% bagi perbezaan tersebut adalah ± 0.20 mm. Hasil kajian ini membuktikan bahawa konsep dan kaedah yang dicadangkan boleh digunakan sebagai alternatif kepada teknik *fringe analysis* yang lain seperti algorithma-algorithma yang berdasarkan transformasian dan algorithma-algorithma yang berdasarkan *phase-shifting* untuk mencapai pengukuran 3D kelajuan tinggi.

SINGLE FRAME PROFILOMETRY WITH RAPID PHASE DEMODULATION ON COLOUR-CODED FRINGES

ABSTRACT

Digital fringe projection profilometry (DFPP) is a non-contact whole-field surface profiling technique. Being able to produce dynamic measurement with high accuracy at video framerates of up to 4000 Hz, this technique is particularly useful in the biomedical field, industrial inspections and cultural heritage preservation. One primary challenge is increasing the measurement speed to achieve higher throughput and higher detectable rates of change. In this work, the applicability of De Bruijn colour-coded sinusoidal fringe projection pattern in achieving single frame profilometry was studied along with phase errors that occur due to gamma nonlinearity and colour crosstalk. Simplification of geometric model by using inherent slanted projection angle in off-the-shelf projector was also studied in this work. Therefore, a corresponding fringe analysis algorithm was developed for De Bruijn colour-coded fringe pattern to circumvent the conventional phase unwrapping techniques which are unreliable and time-consuming. A phase error compensation algorithm and a simplified geometric model were also developed to reduce the phase errors and number of model affliated parameters respectively. Three experiments were carried out to: (i) verify the applicability of the algorithms used in the proposed single-frame profilometry system; (ii) verify the applicability of the proposed phase error compensation algorithm; and (iii) compare the result of the proposed profilometry against the Mitutoyo CRYSTA-Plus M Series 196 coordinate-measuring machine (CMM). The experimental results showed that the proposed profilometry was able to reconstruct objects successfully and consistently using only a single-frame fringe

image. The phase error compensation algorithm was also proven to reduce phase errors at reference level from (1.08 ± 2.32) % to (0.73 ± 0.46) % with a 95% confidence level for 8 iterations on average, producing a visually smoother reconstructed surface. In the comparison against the CMM on the reconstruction of a fan blade curved surface, the mean profile-to-profile differences were consistently recorded as 2.63 mm on average and the confidence intervals of the differences at 95% confidence level were recorded at around ± 0.20 mm. The findings prove that the proposed concept is applicable and provides an alternative method for conventional fringe analysis techniques such as transform-based algorithms or phase-shifting algorithms to advance high-speed 3D profilometry.

CHAPTER 1

INTRODUCTION

1.1 Research Background

Digital fringe projection profilometry (DFPP) is an optical 3D surface profiling technique that uses a projected fringe pattern as a spatial marker. In general, DFPP consists of three main hardware components, i.e. a camera, a projector, and a computer, as shown in Figure 1.1. The fringe patterns are projected by the projector on the object surface at a tilt angle. Due to the tilt angle and the shape of the object surface, the projected fringe pattern is reflected at different angles and captured by the camera. Consequently, as the light of the projected fringe pattern reaches the image sensor of the camera, the acquired fringe pattern appears to be deformed when compared to the ideal fringe pattern acquired at reference plane. Finally, the fringe pattern differences are analysed and converted into 3D coordinates based on the geometric relationship between the placement of projector, camera, and reference plane using the computer. Besides fringe analysis and coordinate conversion, the computer is also used for generating the fringe pattern, sequencing projected fringe patterns, and synchronising the timing between fringe pattern projection and fringe image acquisition. The discussion on DFPP can be separated into several processes, i.e. pattern projection, fringe image acquisition, phase demodulation, phase unwrapping, and triangulation. The process flow of DFPP is illustrated in Figure 1.2. These processes are repeated for every measurement taken.

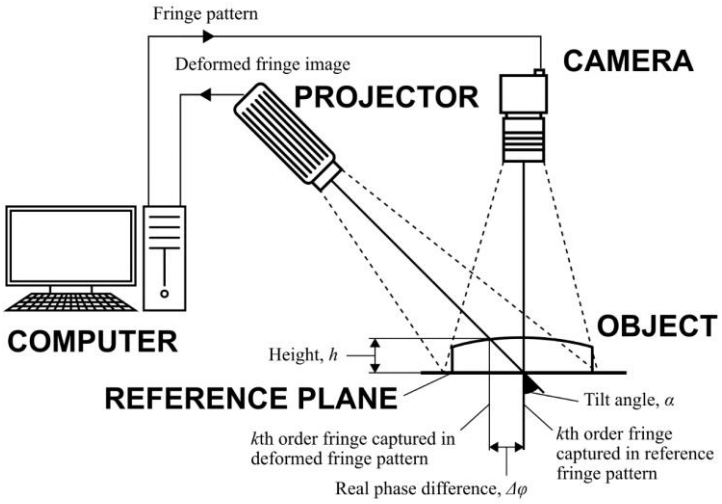

Figure 1.1 Illustration of the general setup of a DFPP system

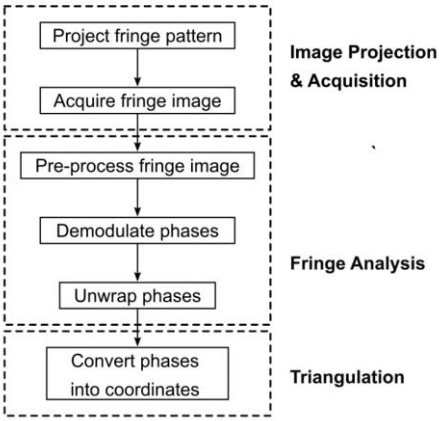

Figure 1.2 Flowchart of overall DFPP processes

The process flow of DFPP starts with the projection of a fringe pattern on the object surface and fringe image acquisition. When the fringe pattern is projected over the object, the fringe pattern deforms according to the shape of the object surface from the viewpoint of the camera, as shown in Figure 1.3. The deformed fringe pattern acquired by the camera is known as the deformed fringe image (Gorthi and Rastogi, 2010). When the fringe pattern is projected directly on the reference plane without objects, the undeformed fringe image acquired by the camera is known as the ideal fringe image. In general, before proceeding with the fringe analysis, the fringe images

have to go through a pre-processing operation in order to filter out image noises and enhance the fringe patterns (El-Hakim et al., 1994). After that, the acquired fringe image is analysed.

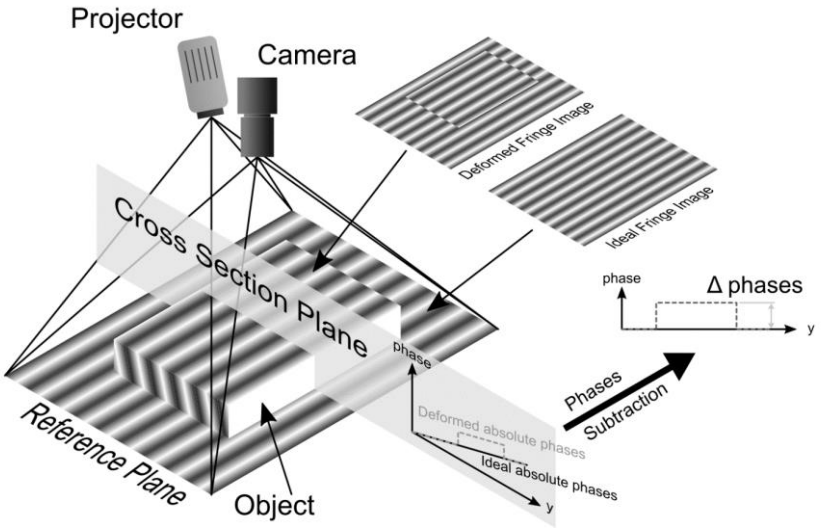

Figure 1.3 Ideal fringe image and deformed fringe image

The discussion on fringe analysis (Gorthi and Rastogi, 2010) can be further separated into two processes, i.e. phase demodulation and phase unwrapping. Firstly, the pre-processed fringe image is fed into the phase demodulation process, which converts the fringe intensity into a phase map (measured in radians). Since the phase demodulation algorithms can only return phases in the range of $[-\pi, \pi]$, these phases are known as wrapped phases (Gorthi and Rastogi, 2010; Van der Jeught and Dirckx, 2016). Figure 1.4 shows examples of the intensity profiles of some common projected fringe patterns and the wrapped phase profiles after demodulation. The fringe pattern used in DFPP are categorised into two main types, i.e. single-frame projection and sequential projection (Van der Jeught and Dirckx, 2016). As suggested by its name, the single-frame projection requires only one frame of the fringe pattern, while sequential projection requires multiple frames of the fringe pattern. Hence, the phase

demodulation algorithm for each type of fringe pattern projection method is also different. Consequently, phase demodulation algorithms are also categorised into two major families, i.e. temporal approaches and spatial approaches (Gorthi and Rastogi, 2010). Basically, temporal approaches are adopted for sequential projection, as they require multiple frames of the fringe images to complete one measurement. Meanwhile, spatial approaches require only one frame of the fringe image to complete one measurement, so this approach is normally adopted for single-frame projection. However, phase demodulation algorithms can only return phases within 2π. This range is too small to reveal the surface shape of the object, so phase unwrapping is needed to unfold the phase map beyond 2π.

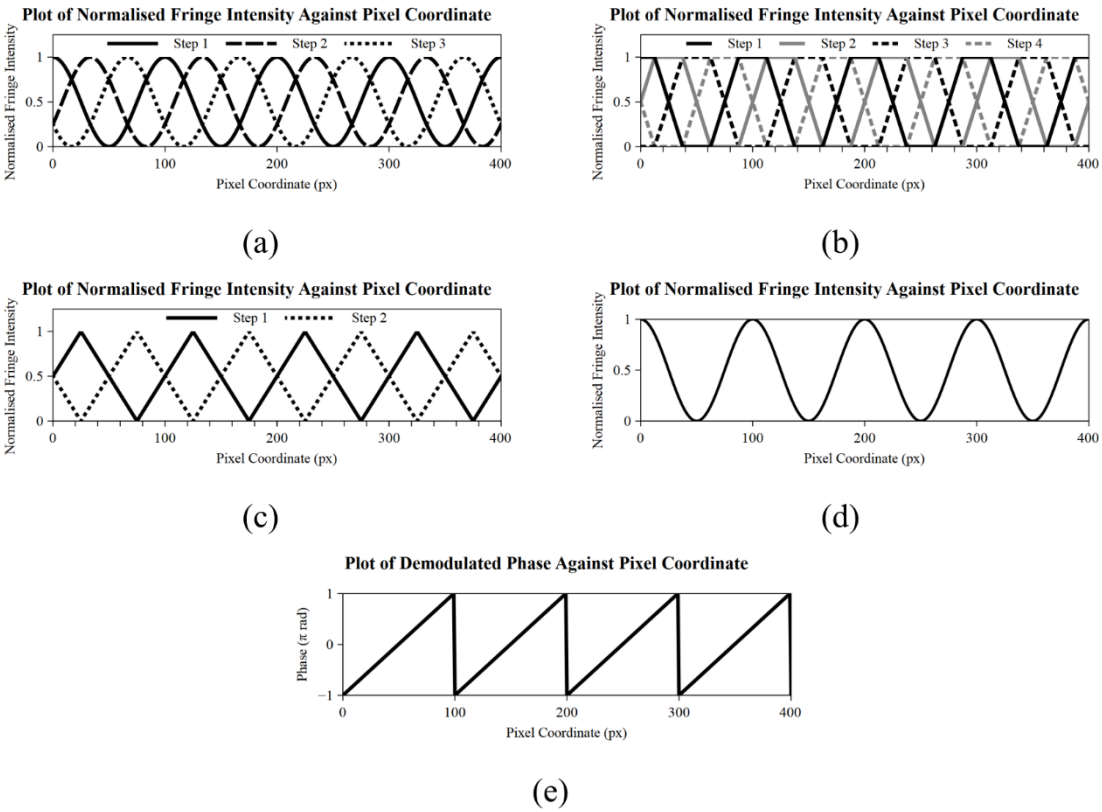

Figure 1.4 Phase demodulation: (a) sinusoidal profile for 3-step phase shifting; (b) trapezoidal profile for trapezoidal phase shifting; (c) triangular profile for triangular phase shifting; (d) sinusoidal profile for Fourier transform demodulation; and (e) wrapped phase profile after demodulation

Phase unwrapping is a process of unfolding the wrapped phase map into a continuous phase map, which is known as the absolute phase map (Gorthi and Rastogi, 2010). After unwrapping, the continuous absolute phase map can go beyond 2π, as shown in Figure 1.5. However, the phase map is not in any usable form, as it is measured in radians and the phase map of the deformed fringe pattern alone cannot reveal the object shape. Therefore, the deformed absolute phase map is compared to the ideal absolute phase map. The difference between these two absolute maps will indicate the relative height of the object surface to the reference plane, as illustrated in Figure 1.3. Finally, by associating the phase map difference with the trigonometry between the placement of the projector, camera, and reference plane, the absolute phase map difference can be converted into a useful form, i.e. 3D coordinates. This phase-to-coordinate conversion process is known as triangulation (Gorthi and Rastogi, 2010). The 3D coordinates will reveal the shape of the reconstructed surface.

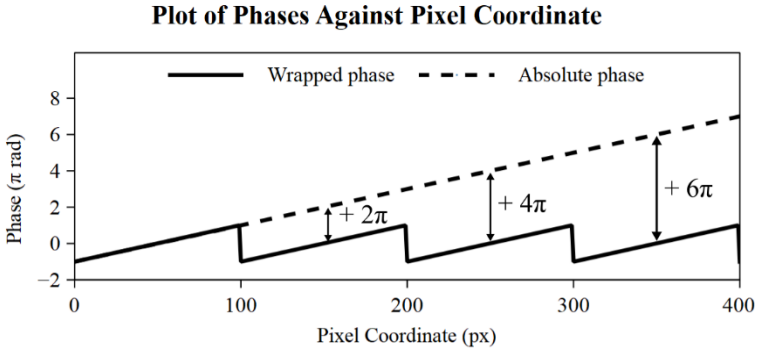

Figure 1.5 Phase unwrapping

DFPP is capable of performing non-contact whole-field measurement at video frame rates (Gorthi and Rastogi, 2010). Unlike the conventional coordinate measuring machine (CMM) such as the 3D laser scanner and probe-type CMM, which have to take a single point measurement at a time (Blais, 2004), DFPP is able to take measurements at multiple points (up to a millions points with a high-definition camera)

simultaneously (Gorthi and Rastogi, 2010). This characteristic enables DFPP to perform much faster than conventional CMM. It can even measure dynamic changes on an object surface (Gorthi and Rastogi, 2010) up to real-time measurement at 15 Hz (Rusinkiewicz et al., 2002), which is an advantage that the conventional CMM does not possess. Besides that, due to its non-contact nature, DFPP is also able to take measurements on soft surfaces without touching the surface subjected to measurement. This advantage enables the application of DFPP on different surfaces, exceeding that of the common probe-type CMM, which requires physical contact. In addition, high-definition cameras, projectors, and high-performance CPUs are widely available at more affordable prices nowadays, owing to advancements in electronics manufacturing, so DFPP has greatly benefited from this trend, as all these components can be utilised in DFPP with minimal modification (Gorthi and Rastogi, 2010). Consequently, DFPP can provide accurate 3D measurement for both static and dynamic surfaces at a more reasonable cost. Therefore, DFPP is now being applied in many fields especially dermatology, encompassing both dynamic and static applications, as listed in Table 1.1 and Table 1.2, respectively.

Table 1.1 Dynamic applications of DFPP in various fields

Application	Reported Works
Biology	
Measurement of a moving object/creature	Cheng et al. (2008); Tan et al. (2000); Wu et al. (2008); Yuan et al. (2001)
3D measurement of live rabbit heart	Wang et al. (2013)
Industrial	
Vibration analysis	He et al. (2006); Yılmaz et al. (2005); Zhang and Su (2005)

Table 1.2 Static applications of DFPP in various fields

Application	Reported Works
Medical	
3D dental measurements	Chen and Huang (2005)
3D imaging of vascular wall deformations	Genovese and Pappalettere (2006)
Human body shape measurement	Hanafi et al. (2005); Lilley et al. (2000); Moore et al. (2006)
Detection and monitoring of scoliosis	Berryman et al. (2008)
Inspection of wounds	Ferraq et al. (2007); Hain et al. (2002)
Skin topography measurement	Jaspers et al. (2006); Lagarde et al. (2002)
Biology	
Face recognition systems	Yagnik et al. (2005); Zhou et al. (2009)
Industrial and Scientific	
Characterisation of MEMS components	Quan et al. (2002)
Refractometry	de Angelis et al. (2000)
Global measurement of free surface	Cobelli et al. (2009); Zhang and Su (2002)
Local wall thickness measurement of formed sheet metals	Weckenmann et al. (2003)
Corrosion analysis	Huang et al. (1999); Jang et al. (2006)
Measurement of surface roughness	Chen and Chang (2008); Spagnolo and Ambrosini (2002)
Reverse engineering	Burke et al. (2002); Hecht et al. (2007); Lin et al. (2005)
Quality control of printed circuit board manufacturing	Hong et al. (2009); Hui and Pang (2008); Yen et al. (2006)
Heat-flow visualisation	Ambrosini and Paoletti (2007)
Art	
Preservation of cultural heritage	Guidi et al. (2001); Sansoni and Docchio (2005); Spagnolo et al. (2004)

As seen in the list of the applications in Tables 1.1 and Table 1.2, the two major advantages of DFPP over conventional CMM techniques are its non-contact nature and its capability to perform dynamic measurement. With the current advancement in

optoelectronics such as ultra-high definition image sensors, ultra-high definition display technologies, high-performance lasers, and LEDs, the non-contact nature of DFPP can be utilised to its fullest potential. Thus, it is important to capitalise on its other advantage, i.e. to increase the measurement speed of DFPP so that a higher throughput is achieved or to increase the maximum detectable rate of change in the dynamic measurement of DFPP. However, there are many challenges in increasing the measurement speed of DFPP. As mentioned before, DFPP can be mainly categorised into two types, i.e. single frame and sequential. Single-frame DFPP requires only one frame of the fringe image while sequential DFPP requires multiple frames of the fringe image. The number of frames of the required fringe images will affect the speed of the data acquisition. In other words, the maximum rate of detectable change on the object surface subjected to measurement is severely limited by the number of required fringe images. Meanwhile, in the subsequent phase demodulation process, spatial approaches generally need a longer time and more computational resources than temporal approaches (Lei et al., 2010; Qian, 2004). This implies that in terms of the speed of the fringe analysis alone, temporal approaches are faster than spatial approaches. Thus, the single-frame DFPP has a fast data acquisition speed but a slow fringe analysis. This means that while single-frame DFPP can perform measurements with dynamic changes on the surface at the video frame rate of the camera, the result of the measurement might not be retrieved instantaneously. Hence, for single-frame DFPP to be adopted in real-time applications, the resolution of measurement may have to be sacrificed (Gorthi and Rastogi, 2010). On the other hand, sequential DFPP has slow data acquisition but a fast fringe analysis. This means that sequential DFPP is more suitable for static measurement. Hence, motion errors (Zuo et al., 2018) could arise when sequential DFPP is applied for dynamic measurement. The motion errors can be

reduced using a higher projection and image acquisition rate or via reducing the number of frames needed per measurement (Wang et al., 2013). However, the minimum number of frames needed per measurement is still more than one frame; thus the measurable maximum rate of change on the surface will be severely limited to the fractions of the projector refreshing rate or camera frame rate (whichever is slower). Therefore, there are significant strengths and weaknesses for both types of DFPP and neither has a significant lead in terms of overall measurement speed.

One study proposed a spatial phase demodulation method with single-frame projection using a direct inverse sine function (Zhang et al., 2013). This method enables both fast data acquisition and phase demodulation. However, it still requires the phase unwrapping process, which is unreliable and complicated, and prone to unwrapping errors, which may lead to incorrect surface reconstruction besides causing a slow processing rate (Zappa and Busca, 2008). Hence, some approaches to modify the projection methods have been introduced to encode more spatial information in the projected pattern such that the phase unwrapping process can be circumvented (Van der Jeught and Dirckx, 2016). These efforts include colour-coded varied intensity fringe patterns such as the De Bruijn colour-coded sinusoidal fringes (Chen et al., 2013; Su, 2007), which can be used to replace varied intensity fringe patterns or varied hue fringe patterns. However, when the colour-coded and varied intensity fringe patterns are used together, the demodulated phase map will contain phase errors that are a result of the gamma nonlinearity effect and colour crosstalk effect. Thus, the accuracy and precision of DFPP will be affected by these phase errors. A solution (Rao and Da, 2015) to these problems has been proposed, but it is based on colour-phase shifting patterns, which are repetitive and cyclic in nature.

Besides that, correcting the projected fringe pattern is difficult because the reported geometric models (Huang et al., 2014; Mao et al., 2007; Takeda and Mutoh, 1983; Xiao et al., 2012) need a tilted projection angle and a high number of model-affiliated parameters. The tilt angle causes inconsistent fringe width, which would be difficult to correct, as the lens configuration and inner dimensions of off-the-shelf projectors are not given to users. The inconsistent fringe width adds more complexity to the phase error compensation, as the error source now includes a tilt angle in addition to existing gamma nonlinearities or colour crosstalk. Furthermore, the more the number of model-affiliated parameters, the higher the difficulty of the calibration processes.

1.2 Problem Statement

Efforts to increase the measurement speed of DFPP have always had to compromise between speed of image acquisition and speed of fringe analysis. A single-frame DFPP, which has a fast image acquisition, may need to sacrifice resolution in real-time applications, as its fringe analysis speed is slow. Meanwhile, sequential DFPP could encounter motion error in dynamic measurements despite having a fast fringe analysis. A single-frame DFPP that uses a direct inverse sine function was proposed by Zhang et al. (2013). This method has a fast acquisition speed and phase demodulation, but still requires phase unwrapping, which is an unreliable, complicated, and time-consuming process that is prone to error. This could lead to incorrect surface reconstruction and measurement (Zappa and Busca, 2008). Colour-coded varied intensity fringe patterns such as De Bruijn's colour-coded sinusoidal fringes (Chen et al., 2013; Su, 2007) can be used to circumvent phase unwrapping, but the demodulated phase map contains inconsistent and unpredictable phase errors due to the gamma nonlinearity effect and colour crosstalk effect, which needs to be further

addressed. Furthermore, the tilted projection angle, which causes inconsistent fringe width, also complicates the phase error compensation. A high number of model-affiliated parameters also increases the number of steps and difficulty of the calibration processes. In order to speed up the overall processes of DFPP, a faster fringe analysis method with a single-frame projection fringe pattern that can bypass phase unwrapping is needed. In-depth research and development by leveraging on the direct inverse sine function and De Bruijn's colour-coded fringe pattern is therefore needed. A simpler geometric model could also help to reduce the complexity of pre-measurement calibration so as to project a more consistent fringe width.

1.3 Objectives

The objectives of this research are as follows:

1. To evaluate the applicability of the De Bruijn colour-coded fringes pattern in DFPP in order to reduce the number of processes and complexity of the fringe analysis algorithm in single-frame projection.

2. To develop and analyse a fringe analysis algorithm that can return an absolute phase map based on the input of the De Bruijn colour-coded fringe image.

3. To develop and analyse a phase error compensation scheme for the De Bruijn colour-coded fringe pattern caused by gamma nonlinearity and colour crosstalk.

4. To develop a simplified image acquisition configuration to solve the geometric model-related problems such as inconsistent fringe width and high numbers of model-affiliated parameters.

1.4 Scope of Study

This research aims to produce a proof-of-concept work for an improved fringe analysis algorithm to reduce the complexity of DFPP processes and increase the overall process speed using single-frame projection. Since it is still in the proof-of-concept stage, the size of the object to be measured is not the main concern of this work. Thus, a midrange industrial camera with close focus zoom lens and an off-the-shelf projector was used to form the profilometry system. The specification of the hardware and the optics geometry limits the object size within 200 mm × 200 mm × 100 mm, to ensure the fringe images acquired were in focus range. Parametric studies (on the scale and dimensions of the pattern fringes or object) and system optimisation (both hardware and software) are beyond the scope of this research.

CHAPTER 2

LITERATURE REVIEW

This chapter provides detailed insight into the main components of the DFPP processes, which were briefly introduced in Chapter 1. The topics reviewed include projection patterns, phase demodulation techniques, phase unwrapping algorithms, encountered phase errors, and geometric models used in triangulation reported in the past. The strengths and weaknesses of each reported technique and/or algorithm and the solutions to the phase errors are discussed in depth in order to provide an overview of the current challenges in the field of DFPP. Some notable review articles that have covered the current progress and challenges of DFPP include Gorthi and Rastogi (2010), who provided a general review of DFPP techniques and Van der Jeught and Dirckx (2016), who discussed the projection patterns used in DFPP.

2.1 Projection Patterns

Fringe projection methods can be categorised into two main types, i.e. single-frame projection and sequential projection. Single-frame projection, also known as single-frame profilometry, projects only one projection pattern image and requires one frame of the deformed fringe image to perform one measurement. On the other hand, sequential projection projects more than one projection pattern image and requires multiple deformed fringe images to perform one measurement. Therefore, sequential projection systems need external circuitries as well as an extra process to synchronise the timing between the fringe pattern projection and acquisition of the respective deformed fringe images, whereas single-frame projection systems can just directly use off-the-shelf projectors and cameras without needing to synchronise them (Gorthi and Rastogi, 2010).

The fringe patterns used in sequential projection are known as sequential projection patterns. Meanwhile, the fringe patterns used in single-frame projection are separated into two families, i.e. greyscale indexing projection patterns and colour-coded projection patterns. The family tree of the projection patterns and the reported works are shown in Figure 2.1 and Table 2.1, respectively.

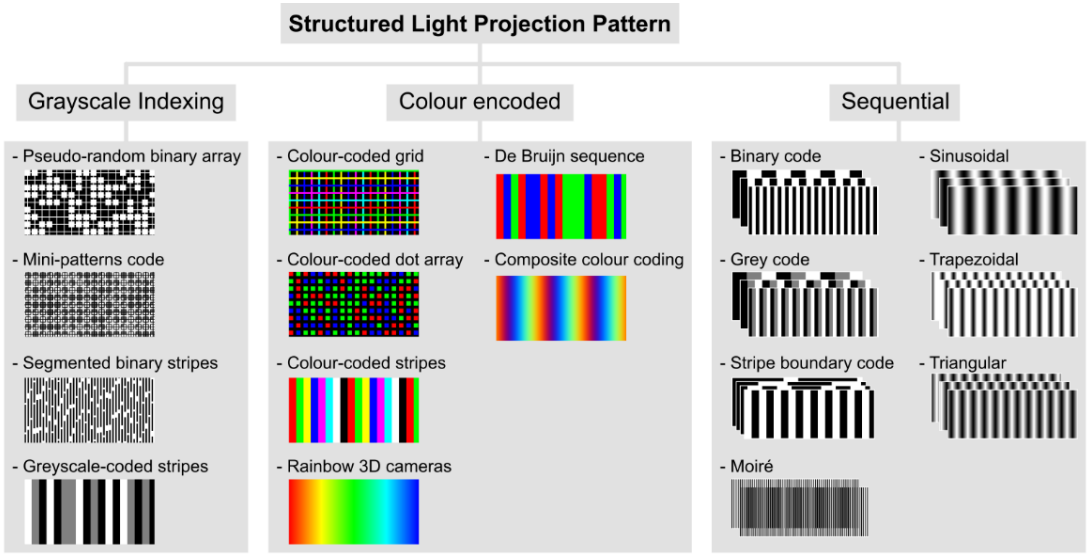

Figure 2.1 Family tree of structured light projection patterns

Table 2.1 List of structured light projection patterns

Patterns	Reported Works
Greyscale indexing	
Pseudo-random binary array	Le Moigne and Waxman (1988); Payeur and Desjardins (2009)
Mini-patterns code	Griffin et al. (1992)
Segmented binary stripes	Maruyama and Abe (1993)
Greyscale-coded stripes	Durdle et al. (1998)

Table 2.1 (Continued)

Patterns	Reported Works
Colour encoded	
Rainbow 3D cameras	Geng (1996); Weinberg et al. (2004)
Colour-coded stripes	Liu et al. (2000)
De Bruijn sequence	Li et al. (2002); MacWilliams and Sloane (1976)
Composite colour coding	Boyer and Kak (1987); Fernandez et al. (2010); Zhang et al. (2006); Zhou et al. (2015)
Colour-coded grid	Petriu et al. (2000); Salvi et al. (2004)
Colour-coded dot array	Desjardins and Payeur (2007); Geng (2011); Payeur and Desjardins (2009)
Sequential	
Binary code	Posdamer and Altschuler (1982)
Grey code	Sato and Inokuchi (1985)
Stripe boundary code	Hall-Holt and Rusinkiewicz (2001); Rusinkiewicz et al. (2002)
Moiré	Benoit et al. (1975); Buytaert and Dirckx (2008); Buytaert and Dirckx (2010); Dirckx et al. (2010); Engelhardt (1991); Meadows et al. (1970); Pirodda (1982); Ryu et al. (2008); Takasaki (1970)
Sinusoidal	Li and Zhang (2017); Stoykova et al. (2013)
Trapezoidal	Huang and Zhang (2006); Zhang and Huang (2004)
Triangular	Jia et al. (2007a); Jia et al. (2008)

2.1.1 Greyscale Indexing Projection Patterns

Greyscale indexing projection patterns are colour-independent patterns that consist of a series of dots (pseudo-random binary array), stripes (segmented binary stripes and grayscale-coded stripes), or coded patterns (mini-patterns code). These dots, stripes, and coded patterns serve as spatial markers for reconstructing the object. The

combination of these features and the neighbourhood of the features will form a unique code, which distinguishes its absolute position via pattern search and matching algorithms.

Due to their colour independent nature, greyscale indexing projection patterns are used to measure surfaces with non-uniform colour distributions. Since they are projected and acquired in greyscale format, the image file size is much smaller because there is only one channel for the greyscale images. In addition, greyscale cameras, which usually have higher actual resolution than a colour camera with a similar pixel count (as a result of colour filter array interpolation (Nakamura, 2005)) can be used for these patterns.

However, the pattern matching algorithms require at least a sub-window of the projected pattern (several pixels to form one recognisable feature) to reveal the absolute position of the object. Hence, the resolution of patterns and their consequent measurement are much lower than the image resolution, as they are not at pixel level. Sometimes, the patterns projected on a surface with discontinuities may not reach the camera sensor due to projection angle, surface reflectivity, and shadows. The missing features in the acquired fringe images will therefore cause unrecognisable features and reduce the robustness and accuracy of measurement.

2.1.2 Colour-Encoded Projection Patterns

Colour-encoded projection patterns use light colour hue instead of light intensity to uniquely map an object's surface. This is seen in the rainbow 3D camera method in which the object is illuminated with a spatially varying colour hue. This pattern establishes a one-to-one correspondence between the projection angle and a particular

colour hue. As a result, it is highly sensitive to the dynamic range and colour resolution of the camera and projector. In contrast to the rainbow 3D camera, colour-coded stripes divide the colour hue into several discrete levels (several specific colours) instead of using the whole range of the colour hue. This makes colour-coded stripes more robust for use on surfaces with non-uniform colour distribution, but the range and resolution of the pattern will be reduced at the same time. In order to cover a large measurement area, the colour-coded stripes have to be repeated, but this repetition also introduces ambiguities. This issue can be solved by arranging the colour stripes according to the De Bruijn sequence. The De Bruijn sequence turns a set of k colour stripes into a fringe pattern of k^n uniquely identifiable stripes given that n contiguous local stripes from the whole sequence are available for template matching. However, like the greyscale indexing patterns, if the stripes were missed due to projection angle, surface reflectivity, and shadow, the template matching may not properly recover the order of colour stripes. Hence, this method is highly sensitive to objects with surface discontinuities.

Apart from colour stripes, colour-coded grids and colour-coded dot arrays work in a way similar to the pseudo-random binary array. With the benefit of having three channels in the image format, these colour-coded patterns can use more than two different colours while the bit depth of the pseudo-random binary array is limited to two. This enables a higher number of unique combinations in the colour-coded patterns than that of the pseudo-random binary array.

Another coloured pattern that takes advantage of the three channels in image format is the RBG image. In a RGB image, it is possible to encode one intensity profile in each channel. As mentioned earlier, the sequential projection system projects one pattern onto the object at a time. By combining three intensity profiles into one

projection image, it is possible to have a single-frame profilometry that can be demodulated using phase-shifting algorithms. This technique is known as composite colour coding. However, this approach is highly vulnerable to colour crosstalk and gamma nonlinearity effects, as the intensity profiles have to be extracted from each channel in order to carry out phase demodulation.

2.1.3 Sequential Projection Patterns

As mentioned above, resolving the unique features in greyscale indexing patterns and colour-encoded patterns often requires complex and computationally intensive template matching algorithms. Besides, the patterns are also very sensitive to surface reflectivity and non-uniform colour distribution. On the other hand, sequential projection patterns are more robust in addressing these issues and provides higher measurement resolution. For example, 18 frames of binary-coded fringe patterns can uniquely describe a measurement area of 512 × 512 pixels. Based on the same concept, grey-coded patterns can generate more code words to cover the same measurement area while projecting less frames of the fringe patterns at discretised intensities. Both binary- and grey-coded patterns are more robust for use against image noise as compared to greyscale indexing patterns and colour-encoded patterns.

Besides the binary and grey codes, there are also digitally generated phase-shifted fringe patterns that use the moiré effect, sinusoidal, trapezoidal, and triangular intensity profiles. Similar to binary and grey codes, these digitally-generated phase-shifted patterns recover their phases through temporal methods. For sinusoidal profiles, the phase is recovered through calculation of an arctangent function. For the moiré projection, a set of dark fringes is projected onto the object surface and overlaid with

another set of dark fringes. Under the moiré effect, these two sets of fringes produce an interference pattern, which can also be converted into phases using the arctangent function. However, the arctangent function calculation is deemed too slow for real-time application. Hence, Huang and Zhang (2006) proposed a three-step phase-shifting algorithm that uses a straightforward intensity ratio calculation and trapezoidal intensity profiles to replace the computationally time-consuming arctangent function and the sinusoidal intensity profiles. Another similar effort was proposed by Jia et al. (2007b), who replaced the sinusoidal profiles and arctangent function with linearly-coded triangular profiles and an intensity ratio calculation. The ideal triangular intensity profiles are characterised by sharp corners. However, the projected and acquired intensity profiles are not perfectly sharp, as they are affected by gamma nonlinearity and image defocus. Consequently, the phases recovered around the peaks and troughs of the profile are erroneous, thus affecting the precision and accuracy of the measurement.

Generally, the sequential projection patterns have higher measurement accuracy and resolution, but require several frames of the fringe images to complete one measurement. Hence, it slows down the measurement speed and causes motion error if the object is not static. This led to the introduction of a sequential projection pattern known as the stripe boundary code, which is immune to motion error (Van der Jeught and Dirckx, 2016). This technique relies on time-codification of the boundaries between binary stripes. By tracking the boundaries between subsequent frames, the method enables identification of the absolute order of the deformed stripes on the object surface even if the object were moving. However, like the greyscale indexing patterns, the resolution of the stripe boundary code is limited to the width of the stripes, which usually spans several pixels.

2.1.4 Hybrid Projection Patterns

Projection patterns with high measurement accuracy and resolution such as sinusoidal, trapezoidal, and triangular intensity profiles have to go through phase demodulation and phase unwrapping to obtain absolute phases (Gorthi and Rastogi, 2010). However, the conventional phase-unwrapping algorithm is time consuming and prone to unwrapping errors (Van der Jeught and Dirckx, 2016). Therefore, recent researchers are now attempting to resolve this issue to increase robustness. One of the efforts include combining the phase-shifting patterns with either greyscale indexing patterns or colour-encoded patterns. These patterns are known as hybrid projection patterns. The reported hybrid patterns and their respective sources are listed down in Table 2.2. For hybrid patterns that combine phase-shifted sinusoidal intensity profiles with binary or grey codes, their main drawbacks—slow measurement speed and prone to motion error—still persist. Fringe patterns that superpose multiple frequencies such as the dual-frequency pattern scheme, multi-frequency pattern scheme, and composite greyscale pattern can be considered as single-frame profilometry. They have fast projection and acquisition speed, but demodulate phases using spatial methods, which are generally computationally intensive and time consuming (Lei et al., 2010; Su and Chen, 2001). Meanwhile, the combination of De Bruijn sequence and sinusoidal intensity profiles is susceptible to colour crosstalk and gamma nonlinearity since RGB channels are used.

Table 2.2 List of hybrid projection patterns

Patterns	Remarks	Reported Works
Binary code + sinusoidal	3 frames of defocused sinusoidal pattern + 3 frames of binary codes	Zhang (2010a)
Grey code + sinusoidal	3 frames of sinusoidal pattern + 4 frames of grey codes	Wang et al. (2011)
Dual-frequency pattern scheme	2 frames of 1D RGB sinusoidal pattern of 2 frequencies	Karpinsky et al. (2014)
Multi-frequency pattern scheme	Multiple frames of a 1D sinusoidal pattern of more than 2 frequencies	Kim et al. (2009); Lei et al. (2015); Wang and Zhang (2011)
Composite greyscale pattern	1 frame of composite pattern, which is superposed from multiple-frequency sinusoidal patterns in 2D	García-Isáis and Alcalá Ochoa (2014); García-Isáis and Alcalá Ochoa (2015); Guan et al. (2003)
De Bruijn sequence + sinusoidal	1 to 3 frames of sinusoidal pattern with colour coded in De Bruijn sequence	Chen et al. (2013); Su (2007)

2.2 Phase Demodulation

Phase demodulation techniques can be categorised into two families, i.e. temporal approaches and spatial approaches. Temporal approaches, also known as phase-shifting algorithms, are usually used to recover phases for sequential projection patterns and hybrid projection patterns. On the other hand, spatial approaches are used to recover phases for single-frame profilometry, which usually employs a single-frame sinusoidal pattern, multiple frequency patterns, and single-frame De Bruijn sequenced colour fringes. The demodulation techniques and their respective sources are listed in Table 2.3.

Table 2.3 List of phase demodulation techniques

Methods	Reported Works
Temporal/Phase Shifting	
Standard *n*-step	Srinivasan et al. (1984)
Double 3-step	Huang et al. (2002)
Hariharan 5-step	Hariharan et al. (1987)
Modified 2+1	Zhang and Yau (2007)
Trapezoidal	Huang et al. (2005)
Triangular	Jia et al. (2007b)
Spatial	
Standard Fourier transform	Chen et al. (2005); Li et al. (2009b); Takeda and Mutoh (1983)
1+1 modified Fourier transform	Guo and Huang (2008)
π-shifted modified Fourier transform	Li et al. (1990)
2D Fourier transform	Lin and Su (1995); Su and Chen (2001)
Windowed Fourier transform	Berryman et al. (2004); Lei et al. (2010); Qian (2004)
Wavelet transform	Gdeisat et al. (2009); Gdeisat et al. (2006); Lei et al. (2010); Li et al. (2016); Li and Yang (2011); Li et al. (2009a); Lim (2010); Zhong and Weng (2004)
Fourier transform + Empirical Mode Decomposition (EMD)	Hawley et al. (2008); Huang et al. (1998)
Fourier transform + Principle Component Analysis (PCA)	Hawley et al. (2008); Huang et al. (1998)
Direct phase recovery algorithm	Zhang et al. (2013)

2.2.1 Temporal Approaches

In pioneering researches, the standard *n*-step phase-shifting algorithm was the most commonly used to demodulate phases for phase-shifted sinusoidal patterns. In the standard *n*-step phase-shifting algorithm, an arctangent function is used to convert intensities in the fringe images into phases. The normal arctangent function can only return phases in the range of -0.5 π to 0.5 π. A 4-quadrant arctangent function can return the phases in the range of -π to π (twice the range of normal arctangent function). Upon the 2π phase discontinuities, phase unwrapping algorithms are required to obtain the absolute phases. The phase unwrapping algorithms are discussed later. The number of steps used in the phase-shifting algorithm is dependent on the intended application. The 3-step phase-shifting algorithm is widely used for real-time or high-speed 3D shape measurements (Huang et al., 2003; Weise et al., 2007; Zhang, 2010b). The three-step algorithm requires minimum fringe images and is the fastest to use. However, this algorithm is also sensitive to different types of phase errors such as phase-shifting errors, gamma nonlinearity errors, and intensity noise (Zuo et al., 2018). The 4-step phase-shifting algorithm is widely used for its relatively high measurement accuracy, low pattern count, and good error tolerance (Zuo et al., 2018). Generally, the higher the step number, the higher the accuracy and tolerance of the algorithm to the phase errors, but also the slower it is in terms of measurement speed.

Huang et al. (2002) proposed a double 3-step phase-shifting algorithm to improve upon the 3-step phase shifting algorithm, which is susceptible to phase errors induced by gamma nonlinearity. However, the method requires three extra fringe patterns to perform the additional 3-step algorithm. Thus, it can significantly reduce nonlinearity error but will use double the acquisition time of a normal 3-step phase-

shifting algorithm. On the other hand, the Hariharan algorithm is a 5-step phase-shifting algorithm that is designed to be insensitive to phase shift errors. Zhang and Yau (2007) proposed a modified 2+1 phase-shifting algorithm to alleviate motion error, which arises when the object moves or changes during measurement. However, since only 2-step phase-shifted fringe images are used, this method is more susceptible to errors resulting from noise and gamma nonlinearity.

As mentioned earlier, there are also phase-shifting patterns with intensity profiles in trapezoidal and triangular shapes. Huang et al. (2005) proposed a trapezoidal phase-shifting pattern along with a respective demodulation technique. The method used intensity ratio directly instead of the arctangent function, which is deemed too slow for real-time applications. Despite using intensity ratio instead of phases, the method still requires phase unwrapping because the periodical nature of the pattern introduces ambiguities. The "vertices" of trapezoidal patterns are very sharp, and thus are sensitive to the intensity blur effect induced by lens defocusing and gamma nonlinearity (Zuo et al., 2018). Jia et al. (2007b) proposed a triangular phase-shifting algorithm, which requires only a minimum of two rather than three patterns to reconstruct the 3D shape of an object. Similar to the trapezoidal phase-shifting algorithm, it also uses the intensity ratio and requires phase unwrapping. Similarly, the sharp "vertices" of the patterns also makes it sensitive to the intensity blur effect induced by lens defocusing and gamma nonlinearity (Zuo et al., 2018).